Supplemental Figure 1

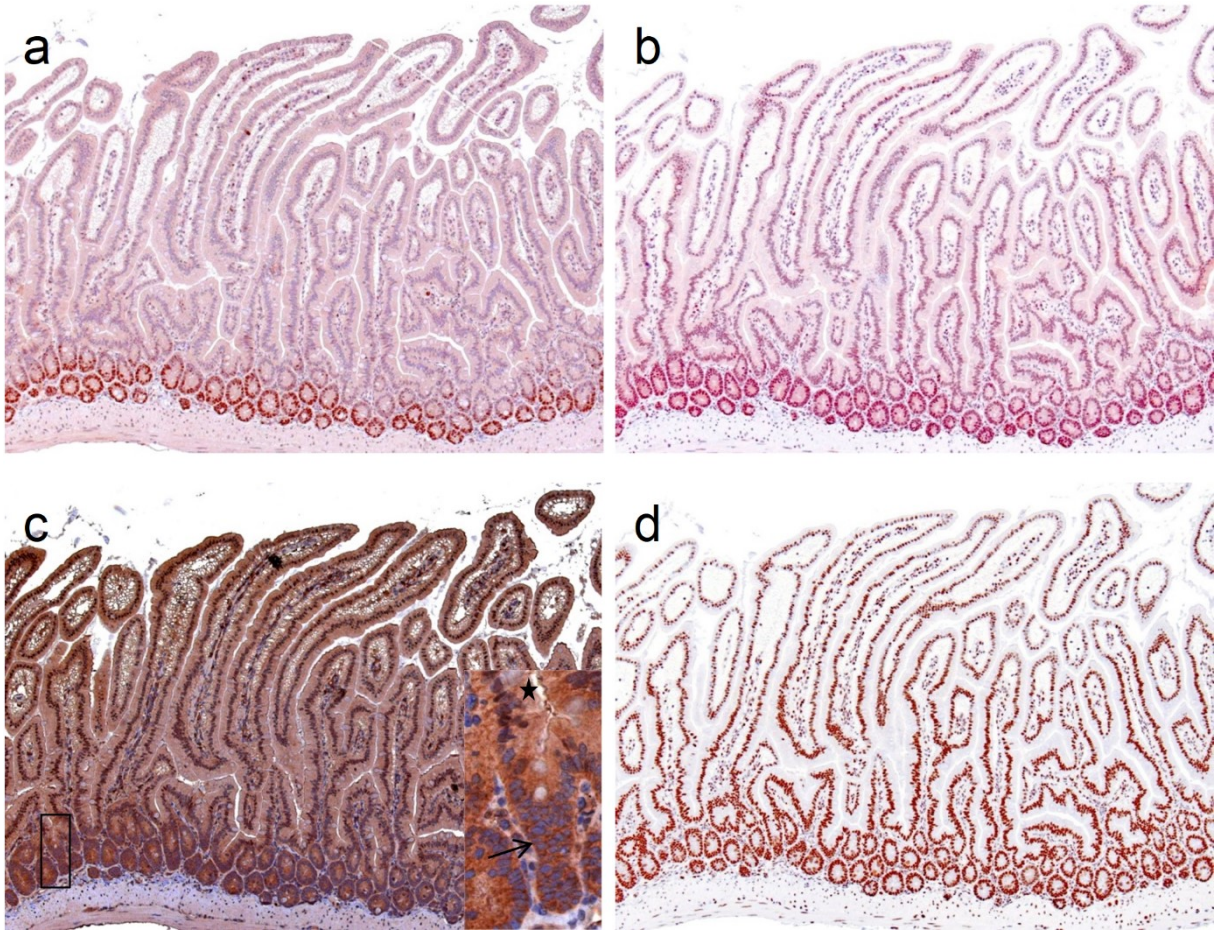

Supplemental Figure 1: c-MYC, SIRT1, NAMPT and DBC1 expression in murine serrated hyperplasia of *Vil-Cre;Braf*$^{LSL-V637E}$ mice.
Immunohistochemical analyses of murine serrated hyperplasia (n= 5) shows that c-MYC (a) and SIRT1 (b) are expressed in the basal third of the crypts. NAMPT expression is restricted to the cytoplasm in intestinal epithelial cells of the crypts and is localized in the cytoplasm and the nucleus of the epithelial cells of the villi (c). Inset shows high magnification of crypts (arrow) and lower part of the villi (asterisks). Nuclear DBC1 displays a homogenous expression pattern along the crypts and villi of the small intestine (d). (Original magnification 100 x, inset 630 x).

Supplemental Figure 2

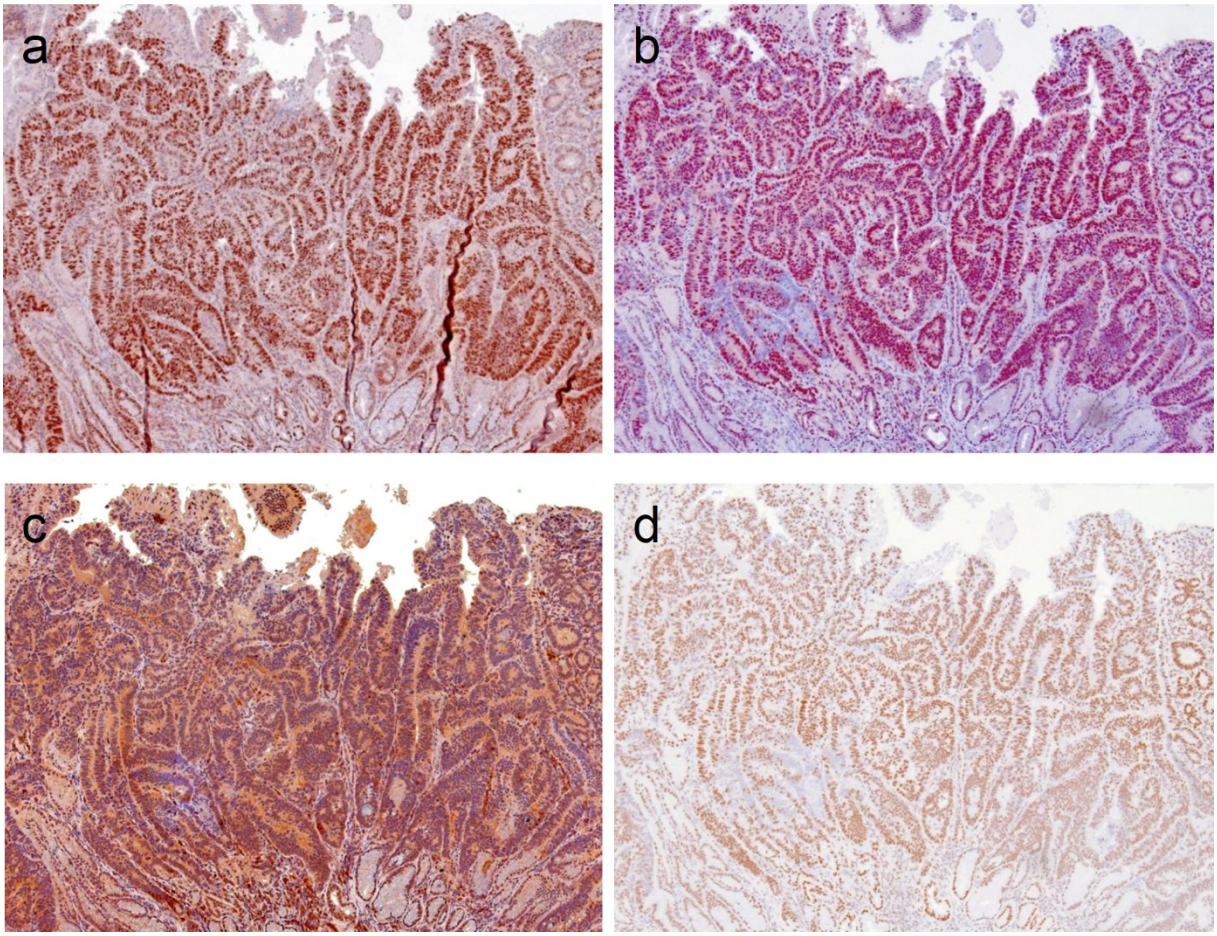

Supplemental Figure 2: High expression of c-MYC, SIRT1, NAMPT and DBC1 in murine serrated adenoma in *Vil-Cre;Braf*$^{LSL\text{-}V637E}$ mice.

Immunohistochemical analyses of murine serrated adenomas with high grade dysplasia (n= 23) shows nuclear c-MYC (a), nuclear SIRT1 (b), cytoplasmic NAMPT (c) and nuclear DBC1 (d) are strongly expressed in the entire dysplastic area. (Original magnification 100 x).

Supplemental Figure 3

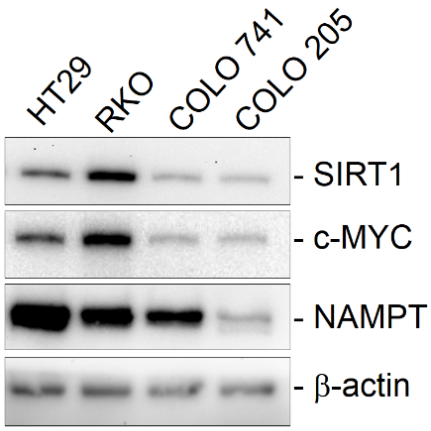

	HT29	RKO	COLO 741	COLO 205
SIRT1	2.7	8.8	2.0	1.0
c-MYC	4.9	15.5	2.5	1.0
NAMPT	3.7	2.0	1.8	1.0

Supplemental Figure 3: Protein expression of SIRT1, c-MYC and NAMPT in *BRAF*-mutant cancer cell lines.
SIRT1, c-MYC and NAMPT expression were analyzed by immunoblot in HT29, RKO, and COLO 205 colorectal cancer cell lines with β-actin serving as loading control. (The *BRAF*-mutant COLO 741 cell line has formerly been classified as a colorectal cancer line, and is now considered a pelvic melanoma metastasis (Medico et al., 2015)). Protein expression was quantified using densitometry. The table depicts arbitrary expression values relative to the expression of COLO 205 cells, which was set as 1.

Supplemental Figure 4

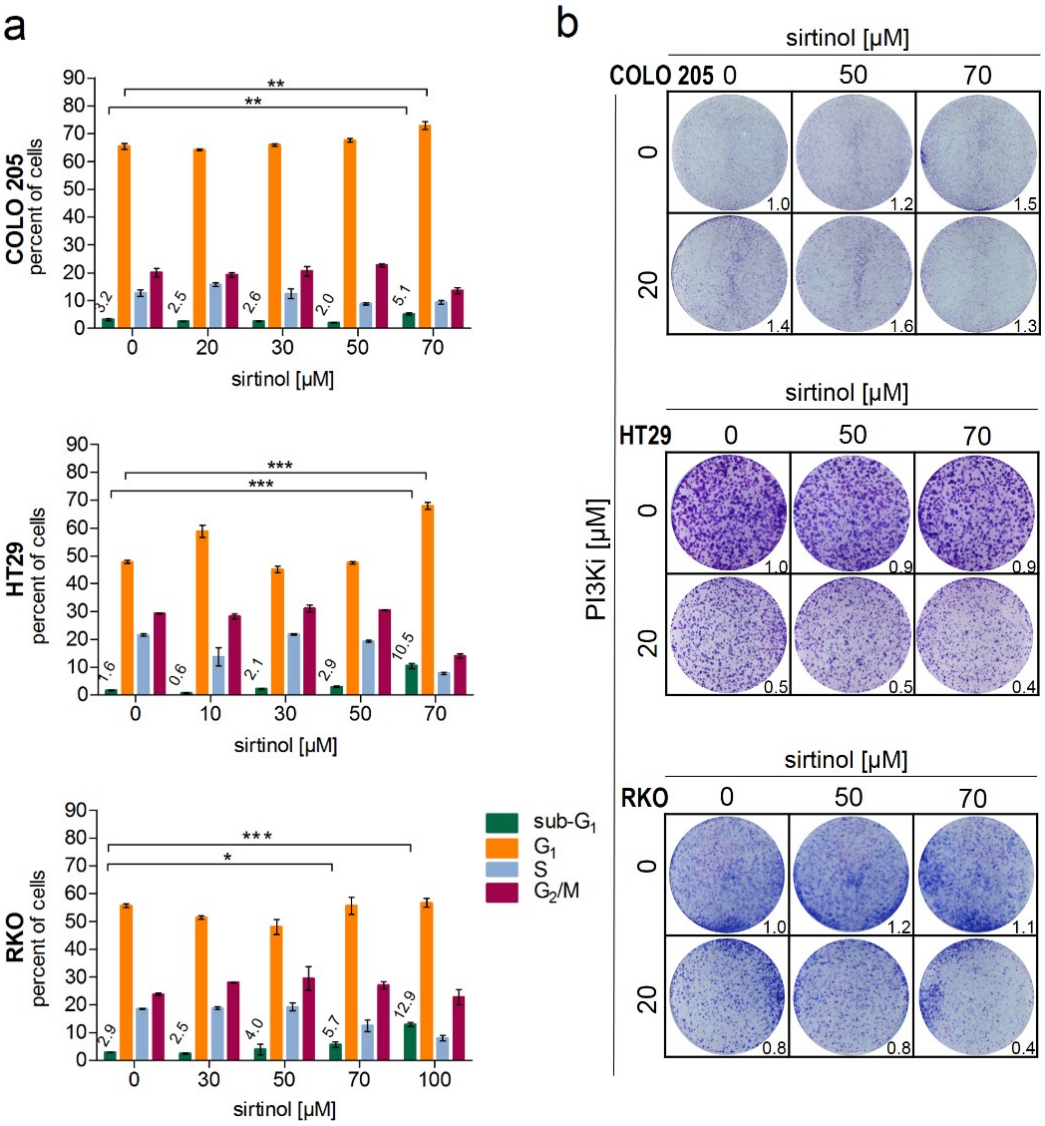

Supplemental Figure 4: SIRT1 inhibition slightly induces apoptosis and SIRT1 inhibition combined with a PI3K inhibitor reduces colony growth of *BRAF*-mutant CRC cell lines.

(a) The indicated cell lines were exposed to increasing concentrations of the SIRT1 inhibitor sirtinol, or the solvent (0) for 2 days. DNA content of biological triplicates was determined by FACS analyses with percentages and standard deviation of sub-G_1, G_1, S and G_2/M cell cycle phases depicted. Percentage values of sub-G_1 fractions are given as indicated. Statistical analysis was done by one-way ANOVA followed by Tukey's post-hoc test. * $p < 0.05$, ** $p < 0.01$, *** $p < 0.001$.

(b) Colony-forming assays document cell viability upon single and combined pharmacological inhibition of PI3K and SIRT1 in the indicated cell lines. Clonogenic assays were performed after two weeks inoculation of sirtinol, or solvent (0) as single agent (upper row), or its combination with the PI3K inhibitor LY294002 (lower row) at the indicated concentrations. Image J software was used for quantification of Giemsa stained colonies. The area covered by untreated cells was defined as 1. Ratios of inhibitor treated cells versus untreated cells are given in the lower right corners.

Supplemental Figure 5

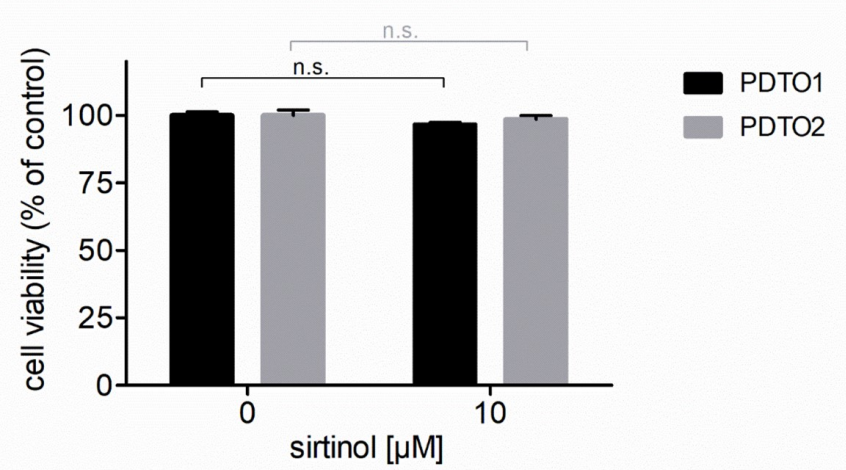

Supplemental Figure 5: Viability of primary BRAF(V600E)-expressing tumor organoid cultures upon inhibition of SIRT1.
Colony-forming assays of two primary BRAF(V600E)-expressing patient derived tumor organoid cultures (PDTO1 and PDTO2) shows that sirtinol had no effect on cell viability. Single tumor organoid cells plated in 3-D matrigel were inoculated with the indicated concentration of either sirtinol or the solvent (DMSO) 48 hours after seeding. Cell viability of tumor organoid cultures was assessed after 7 days (PDTO1) and 5 days (PDTO2) via indirect luminometric detection of the cellular ATP content (3-D Cell TiterGlo assay). The experiment was performed in biological triplicates. Error bars indicate standard deviation. Statistical analyses of two experimental groups was done by t-test. n.s.: not significant

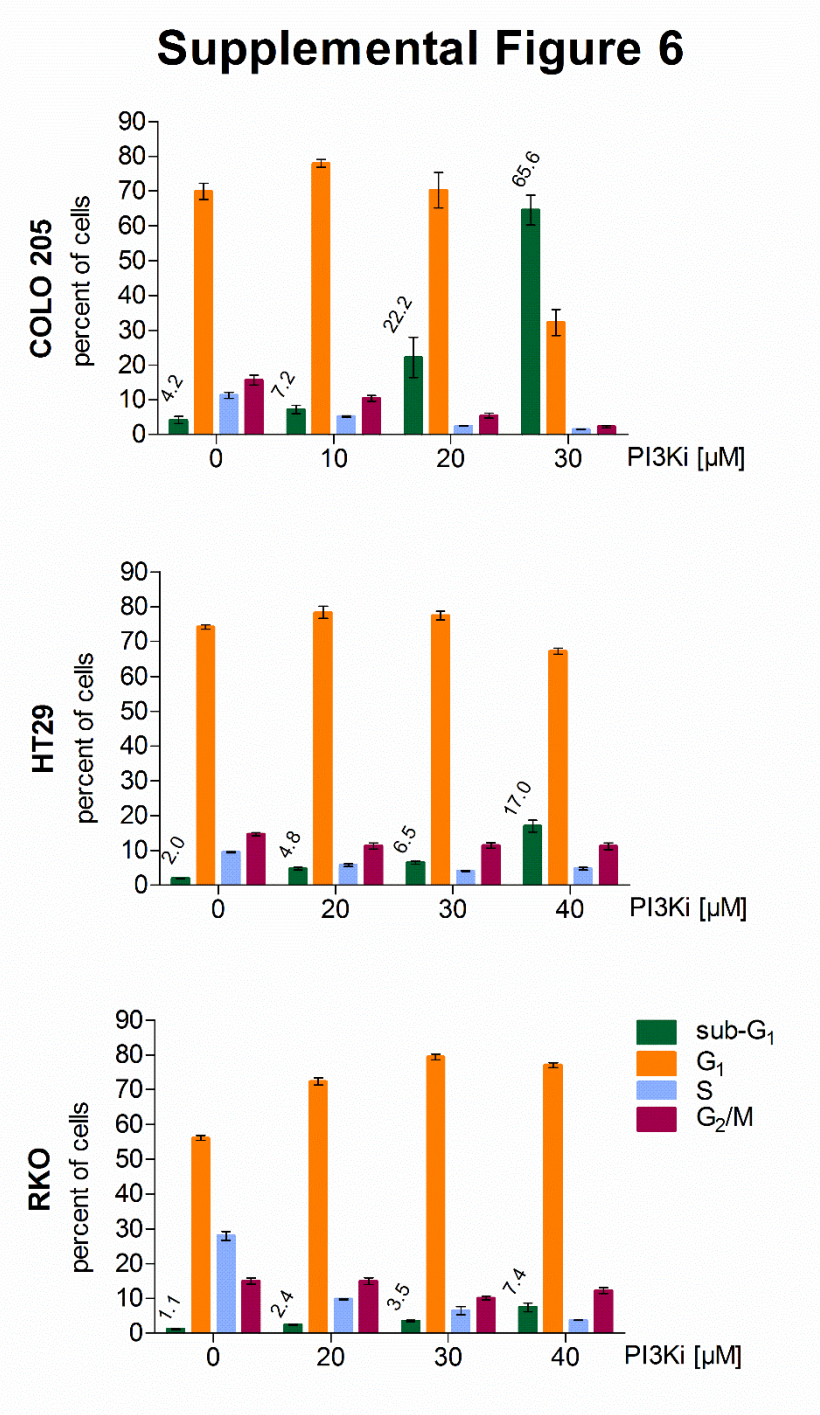

Supplemental Figure 6: Inhibition of PI3K in *BRAF*-mutant human colorectal cancer cell lines.

Increasing concentrations of the PI3K inhibitor LY294002 were added to the indicated cell lines for two days, followed by DNA content analysis using propidium iodide staining. Percentages of sub-G_1, G_1, S and G_2/M cell cycle phases are depicted. Percentage values of sub-G_1 fractions are given as indicated.

Supplemental Figure 7

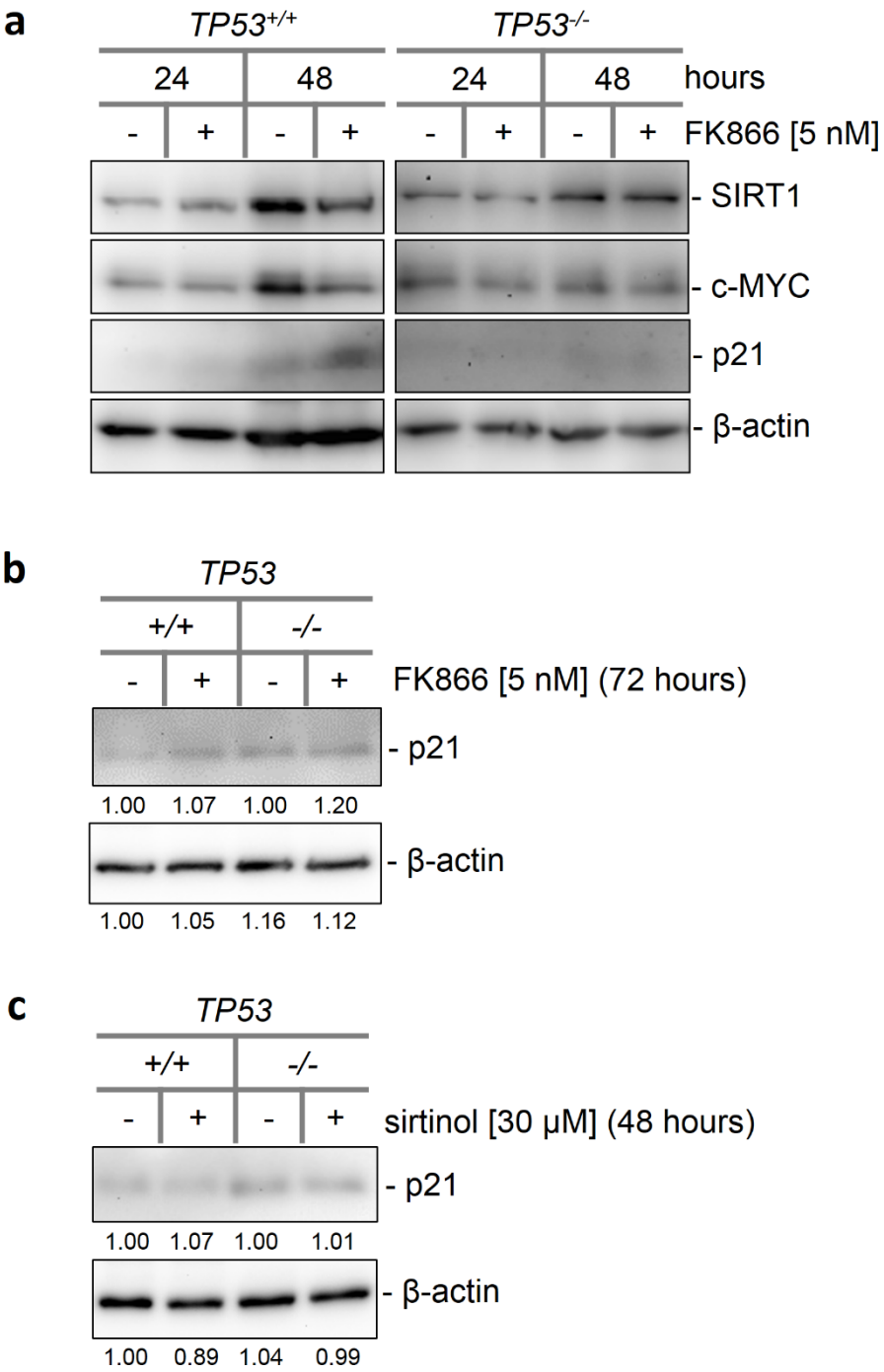

Supplemental Figure 7: Protein expression changes associated with pharmacological interference with the c-MYC-NAMPT-SIRT1 positive feedback loop in *BRAF*-mutant CRC cell lines.
Immunoblot analysis of SIRT1, c-MYC and p21 expression in RKO *TP53*$^{+/+}$ and RKO *TP53*$^{-/-}$ CRC cells inoculated with FK866 [5 nM] (a, b), or sirtinol [30 μM] (c) for the indicated times. β-actin served as loading control.